

Coexistence of different charge states in Ta-doped monoclinic HfO₂: Theoretical and experimental approaches

M. A. Taylor,¹ R. E. Alonso,^{1,*} L. A. Errico,^{1,2} A. López-García,¹ P. de la Pesa,³ A. Svane,⁴ and N. E. Christensen⁴
¹*Departamento de Física, Instituto de Física La Plata (IFLP, CCT-La Plata, CONICET-UNLP), Facultad de Ciencias Exactas, Universidad Nacional de La Plata, Casilla de Correo 67, 1900 La Plata, Argentina*
²*Universidad Nacional del Noroeste Bonaerense (UNNOBA), Monteagudo 2772, Pergamino, CP 2700, Buenos Aires, Argentina*
³*Instituto de Magnetismo Aplicado, UCM-ADIF-CSIC, P.O. Box 155, 28230 Las Rozas, Spain*
⁴*Department of Physics and Astronomy, Aarhus University, DK-8000 Aarhus C, Denmark*
 (Received 18 August 2010; published 14 October 2010)

A combination of experiments and *ab initio* quantum-mechanical calculations has been applied to examine hyperfine interactions in Ta-doped hafnium dioxide. Although the properties of monoclinic HfO₂ have been the subject of several earlier studies, some aspects remain open. In particular, time differential perturbed angular correlation spectroscopy studies using ¹⁸¹Ta as probe atom revealed the coexistence of two hyperfine interactions in this material but an explanation was only given for the more populated one. Until now, no models have been proposed that explain the second interaction, and it has not yet been associated with a specific crystallographic site. In this work, a detailed study of the different charge states for the impurity-probe atom (Ta) was performed in order to understand the second interaction observed in Ta-doped monoclinic HfO₂. The combination of experiments and theory suggests that two different charge states coexist in this compound. Further, *ab initio* calculations predict that, depending on the impurity charge state, a sizeable magnetic moment can be induced at the probe site. This is confirmed by a new analysis of experimental data.

DOI: [10.1103/PhysRevB.82.165203](https://doi.org/10.1103/PhysRevB.82.165203)

PACS number(s): 71.15.Mb, 76.80.+y, 71.20.Nr

I. INTRODUCTION

Hafnium dioxide has attracted much attention due to its potential technological applications. HfO₂ is a wide-band-gap semiconductor that crystallizes in a monoclinic structure (*m*-HfO₂) at room temperature. It transforms to a tetragonal structure at moderately elevated temperatures and to a cubic structure at higher temperatures. HfO₂ is characterized by a high melting point, high chemical stability, and a large dielectric constant. In its various forms and with the addition of small amounts of impurities, it has applications ranging from solid oxide fuel cell electrolytes to catalyst substrates, and protective coatings (see Ref. 1 and references therein). More recently, ferromagnetism was observed in pure HfO₂ thin films, a result of interest to the field of spintronics.²

Time differential perturbed angular correlation (TDPAC) spectroscopy is a powerful technique to study hafnium compounds. To perform a TDPAC experiment, a suitable probe isotope (generally an impurity) must be introduced adequately in the system under study. In the case of Hf compounds, the ¹⁸¹Hf(\rightarrow ¹⁸¹Ta) probe can be obtained by neutron irradiation of the naturally occurring ¹⁸⁰Hf isotope. The small [parts per million (ppm)] concentration of radioactive tracer atoms necessary to perform the experiment does not influence the macroscopic properties of the matrix. Additionally, in comparison with other nuclear techniques such as Mössbauer spectroscopy, the sensitivity of TDPAC does not depend on a Debye-Waller factor allowing to determine properties or effects occurring at high temperatures. For these reasons, HfO₂ has been extensively studied by means of TDPAC.³

The TDPAC technique provides a high-resolution determination of quadrupolar electric, dipolar magnetic hyperfine interactions, or a combination of both.⁴ The electric quadru-

polar interaction is essentially given by the product of the nuclear quadrupole moment, Q , characteristic of a given nuclear state of spin I , and the electric field gradient (EFG) at the nuclear site. Q is 2.36₅ b for the sensitive TDPAC state of ¹⁸¹Ta.⁵ The measured quantity is the nuclear quadrupolar frequency ω_Q , which is given by $\omega_Q = eQV_{ZZ}/[4I(2I-1)\hbar]$, where V_{ZZ} is the major component of the diagonalized EFG tensor. The EFG tensor is completely specified by V_{ZZ} , together with the asymmetry parameter $\eta = (V_{XX} - V_{YY})/V_{ZZ}$. The magnetic hyperfine interaction is caused by the coupling between the magnetic field produced by the electron spin and the orbital currents at the probe site and the magnetic moment of the nucleus.⁴ The experimentally observed quantity is in this case the precession frequency $\omega_L = g_N \mu_N B_{hf}/\hbar$, where g_N denotes the nuclear g factor and μ_N is the nuclear magneton.⁶ B_{hf} is the magnetic hyperfine field, which is a fingerprint of the magnetic configuration and the spin polarization near and at the probe nucleus. Whereas pure quadrupolar and/or pure magnetic interactions have been extensively observed using TDPAC, cases of combined electric and magnetic interactions (CEMIs) in which the quadrupolar electric and the dipolar magnetic interactions are of the same order of magnitude are scarce in the literature.^{7,8} In the case of a CEMI, the experimentally observed parameters are the quadrupole frequency ω_Q , the asymmetry parameter η , the magnetic frequency ω_L and the Euler angles β , γ which describe the relative orientation of the magnetic hyperfine field and the EFG tensor.

All published TDPAC studies of Ta-doped *m*-HfO₂ reported in the literature refer to a hyperfine interaction (HFII) characterized by a V_{ZZ} of about 13.7×10^{21} V/m² and an asymmetry parameter η of about 0.35 at 300 K.^{3,9} This interaction was assigned to (¹⁸¹Hf \rightarrow)¹⁸¹Ta substitutionally located at the cation sites of *m*-HfO₂. An *ab initio* study on

Ta-doped m -HfO₂ performed in Ref. 1 showed that Ta atoms induce a donor impurity level close to the conduction band of m -HfO₂. By comparing the calculated EFG values with the experimental results it was confirmed that HF11 corresponds to Ta probes located at cationic sites and that the impurity level is ionized (empty) at 300 K.

The experimental results showed that, in addition to HF11, there exist a second interaction in m -HfO₂. Ayala *et al.*⁹ reported a second interaction in coarse grained m -HfO₂ characterized by high V_{ZZ} and η values. Forker *et al.*³ investigated the structure, phase transformations, grain growth, and defects of coarse-grained and bare nanoparticles of m -HfO₂ synthesized in a microwave plasma. The authors found that, in addition to the well-known HF11, a second component involving 20–30 % of the probe nuclei appeared in the ¹⁸¹Ta PAC spectra. The fitted parameters are similar to those reported in Ref. 9. The temperature dependence of this component was reproduced by assuming that Ta impurities in hafnia may trap electrons at low temperatures. This second interaction (hereafter denoted HF12) was never assigned to a regular crystallographic site.

In order to understand the origin of HF12 we performed in this work a detailed study of the electronic and structural properties of Ta-doped HfO₂ for different charge states of the impurity-host system. Since *ab initio* calculations showed that impurities can leave unpaired electrons that can lead to a net magnetic moment,¹⁰ spin-polarized calculations were carried out. The theoretical predictions were compared with a new analysis of the TDPAC experiments reported in Ref. 3.

II. METHOD OF CALCULATION

The calculations were performed with the *ab initio* full-potential linear augmented plane wave plus local orbital (APW+lo) method¹¹ in a scalar relativistic version, as implemented in the WIEN2K code.¹² For the simulation of the diluted Ta impurity, the supercell (SC) scheme was employed following the general guidelines of our previous work.¹ Calculations were made for a periodic arrangement of eight unit cells of m -HfO₂. The resulting 96-atom SC has dimensions $a'=2a=10.234$ Å, $b'=2b=10.3508$ Å, and $c'=2c=10.583$ Å. One Hf atom of the SC was replaced by one Ta atom. With this arrangement, Ta substitution represents about 3 at. % doping. Although this Ta concentration is large compared with parts per million dilution in the samples used in the TDPAC experiments, the choice of the 96-atom SC keeps the Ta atoms sufficiently far from each other (10.3 Å) to avoid significant interactions between impurities. In some cases calculations were performed using cells with 192 atoms ($a'=2a=10.234$ Å, $b'=2b=10.3508$ Å, and $c'=4c=21.166$ Å) and 324 atoms ($a'=3a=15.351$ Å, $b'=3b=15.5262$ Å, and $c'=3c=15.8745$ Å), respectively. The 324 atom SC is the largest SC we could use, maintaining the accuracy of the calculations.

In all cases we used the local spin-density approximation (LSDA, Ref. 13) and the exchange-correlation potential given by Wu and Cohen.¹⁴ The energy cut-off criterion was $R_{mt}K_{MAX}=7$ ($R_{mt}K_{MAX}=6$ for the 324-atom SC), R_{mt} being the smallest muffin-tin radius and K_{MAX} the largest wave

number of the basis set. The number of k points was increased up to 100 to check the convergence of the results. Bond lengths, EFG components, and energy differences between spin-polarized and nonspin-polarized calculations are well converged for the employed parameters. Details of the calculation of the EFG within this code are described in the works of Schwarz *et al.*¹⁵ Relaxation of all the internal atomic positions, that is, the displacements of all the atoms in the SCs were considered.

As shown in a previous work,¹ the presence of the Ta impurity induces a partially filled impurity band at the bottom of the conduction band. These impurity states are spatially located at the Ta atom and its oxygen nearest neighbor (Onn). As it was demonstrated in Refs. 1, 16, and 17, the charge state of the impurity can modify the electronic structure around the impurity. This change can strongly affect the structural distortions and the EFG. In a first scenario, it was assumed that a neutral Ta substitutes Hf in m -HfO₂ and remains in a +4 valence state (henceforth “neutral charge state,” $q=0$). In this case, the impurity state located at the Fermi levels are partially occupied (see Ref. 1). Secondly, calculations removing one electron from the whole system ($q=+1$) were performed, this case is referred to as “charged state” in which the impurity state is empty. The charge imbalance is compensated by adding a uniformly distributed charge of opposite sign in the SC.

III. RESULTS AND DISCUSSION

In Table I we present the calculated results for the relaxed Ta-Onn bond lengths and for the EFG at the Ta site. Comparing the new results with those reported in Ref. 1, it can be seen that the effect of the relaxation of the second and further neighbors do not affect significantly neither the Ta-Onn bond lengths nor the EFG.

Table II shows the experimental values of the hyperfine parameters reported in Ref. 3. Comparing the calculated EFG values of Table I and the experimental ones of Table II, it can be seen that the agreement theory-experiment is remarkable for both charge states. As it was discussed in Ref. 1, HF11 is related to Ta in a regular cationic site of the monoclinic phase with the probe in a charged state. The other interaction also corresponds to a Ta in the cationic site but in this case the impurity energy level introduced by the Ta remains occupied by one electron. In other words, the Ta impurity acts as a trapping site. Coexistence of different charge states was also found for Cd impurities in oxides by a combined TDPAC experimental and *ab initio* theoretical study of Cd-doped SnO (Ref. 18) and in TiO_{2- δ} .¹⁹ This indicates that the coexistence of different charge states in doped or nonstoichiometric oxides may be rather usual.

For some systems (such as Cd complexes in Si and Ge) calculations performed with the Korringa-Kohn-Rostoker-Green’s-function approach have predicted a local magnetic moment that depends on the charge state of the impurity.¹⁰ In effect, in a simple picture, a magnetic signal could be observed whenever a localized state is occupied by a single electron. Therefore, we performed spin-polarized calculations in the 96-atom SC for both charge states. In the case of

TABLE I. Final distances (in Å) from the Ta impurity to its seven Onn for the different calculations performed with the 96-atom cell and compared with those for pure m -HfO₂. Calculated principal EFG component, V_{ZZ} , in units of 10^{21} V/m² and asymmetry parameter η at the Ta impurity site in m -HfO₂ are also reported.

$d(\text{Ta-Onn})$	Unrelaxed structure	$q=0$		$q=+1$	
		LDA	GGA	LDA	GGA
$d(\text{Ta-O1})$	2.03	1.99	2.00	1.95	1.96
$d(\text{Ta-O2})$	2.07	2.02	2.02	1.97	1.98
$d(\text{Ta-O3})$	2.13	2.06	2.05	2.06	2.06
$d(\text{Ta-O4})$	2.14	2.11	2.11	2.06	2.07
$d(\text{Ta-O5})$	2.17	2.12	2.11	2.07	2.08
$d(\text{Ta-O6})$	2.23	2.19	2.20	2.18	2.17
$d(\text{Ta-O7})$	2.25	2.20	2.20	2.19	2.18
$V_{ZZ}(\text{Ta site})$		+20.0	+21.4	+13.7	+13.9
$\eta(\text{Ta site})$		0.42	0.40	0.33	0.30

the charged cell ($q=+1$) there is an even number of electrons while the neutral cell has an odd number of electrons. Thus, in principle, this last case should be the better candidate to present magnetism due to the possibility of an unpaired spin moment. The results of the spin-polarized calculations are shown in Table III. In the case of the charged cell we did not find a magnetic solution, while in contrast, APW+lo predicts spin polarization for the case $q=0$.

The total and Ta d and O p partial density of states (DOS) for the spin-polarized and the nonspin-polarized solutions are shown in Fig. 1. In the case of the nonspin-polarized calculation the Ta d states are centered close to the Fermi level (E_f). As can be seen, the impurity state below the E_f has important Ta d_{z^2} and Ta $d_{x^2-y^2}$ orbital contributions. The effect of spin polarization is to push the main part of the d_{z^2} levels above E_f . This shift produces a strong occupation asymmetry, the occupied part being predominantly of $d_{x^2-y^2}$ character, with small admixtures of d_{z^2} , and d_{xy} symmetries in the majority spin channel. As a result, the system becomes half metallic and the net magnetic moment is $1.0 \mu_B$ ($0.35 \mu_B$ in the Ta sphere).

Total-energy calculations predict that the energy difference $\Delta E = E_{sp} - E_{nsp}$ is -0.05 eV (where E_{sp} and E_{nsp} are the total energy of the spin-polarized and nonspin-polarized cases, respectively), showing that the spin-polarized cell is the energetically more stable. The use of the SC method

(with an unrealistically high Ta concentration compared with the experimental ppm density) produces a broadening of the impurity state. Thus, larger SCs were studied in order to investigate the influence of the localization of the impurity state on the magnetic solution. Calculations were performed using the 192-atom SC (TaHf₆₃O₁₂₈) and 324-atom SC (TaHf₁₀₇O₂₁₆) described in Sec. II and considering $q=0$ and $q=+1$. The results obtained for V_{ZZ} and η for both SCs are shown in Table III. As expected, the hyperfine parameters are very similar to those determined for the 96-atom SC.¹ Again, a net magnetic moment of $1.0 \mu_B$ ($0.35 \mu_B$ in the Ta muffin-tin sphere) was found for $q=0$. The energy difference between spin-polarized and nonspin-polarized calculations favored the spin-polarized case by -0.13 eV (192-atom SC) and -0.12 eV (324-atom SC).

The present calculations show that the experimentally determined hyperfine interactions can be attributed to two different charge states of the probe atom. Moreover, HFI2 could have a combined quadrupole electric and dipolar magnetic character. Up to now, no evidence of this kind of combined interaction was found in the literature for Ta-doped HfO₂. When the perturbation is caused by a CEMI in addition to V_{ZZ} and η , a magnetic frequency ω_L must be taken into account.³ Assuming that the second interaction is described by the predicted combined electric and magnetic interaction (hereafter denoted HFI2C), a new fit was performed on an

TABLE II. Electric field gradient main component V_{ZZ} , asymmetry parameter η , relative frequency distribution ($\Delta\delta/\delta$), and magnetic hyperfine field, B_{hf} , characterizing the hyperfine interaction observed in TDPAC experiments in m -HfO₂ (Ref. 3). In order to derive V_{ZZ} from ω_Q we used the value $Q(^{181}\text{Ta}) = 2.365$ b (Ref. 5).

Model for fitting	Interaction	Relative intensity (%)	V_{ZZ} (10^{21} V/m ²)	η	$\Delta\delta/\delta$ (%)	B_{hf} (T)
Pure electric quadrupolar (Ref. 3)	HFI1	75	13.90 ₄	0.345 ₅	7 ₁	
	HFI2	25	23 ₂	0.3–0.4	40 ₁₀	
CEMI (this work)	HFI1	82	13.56 ₂	0.36 ₁	6 ₁	
	HFI2C	18	22.7 ₃	0.47 ₂	1 ₁	11.2 ₃

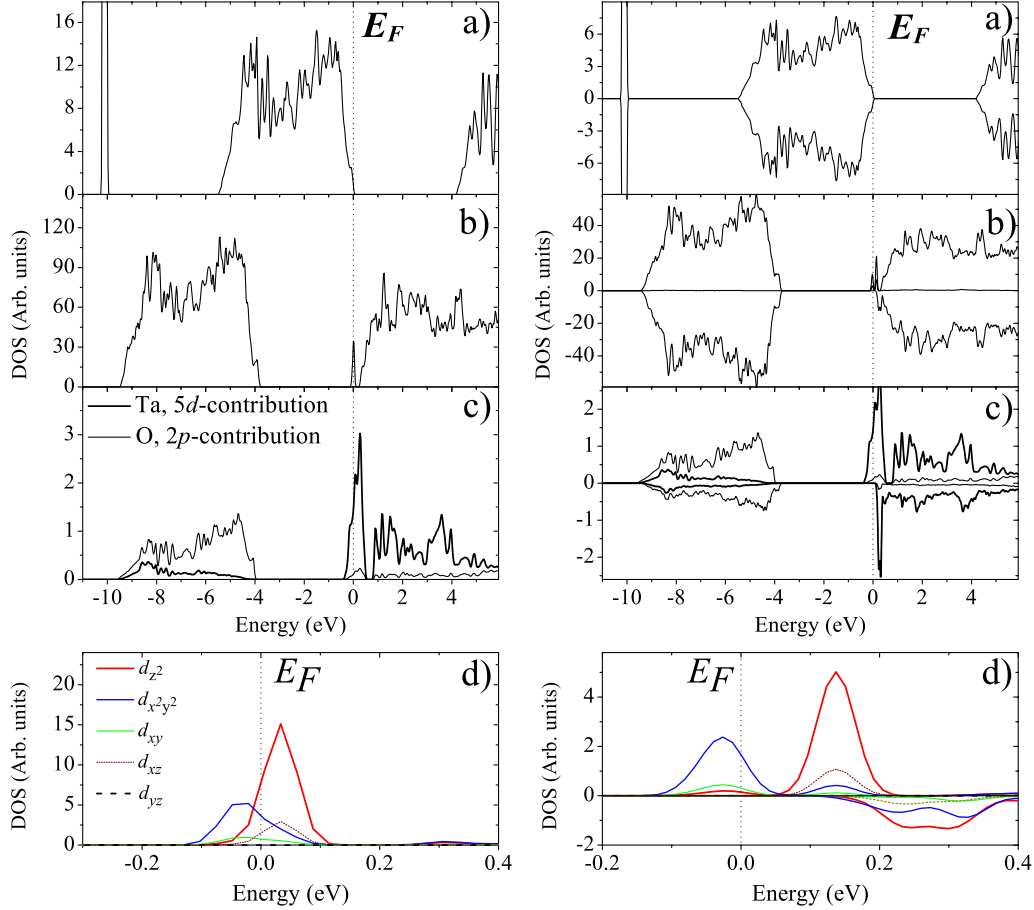


FIG. 1. (Color online) DOS of (a): pure m -HfO₂; (b): Ta-doped m -HfO₂; (c): partial DOS of Ta d and O p characters; and (d): orbital-resolved partial DOS of Ta d states. The calculations are LSDA calculations for the relaxed system TaHf₃₁O₆₄ (96-atom SC) for $q=0$. Left panel shows the nonspin-polarized calculation and right panel the spin-polarized calculation. Energies are referred to the Fermi level (E_F), and on the right, negative values of the DOS refer to minority spin and positive value to majority spin. Note the change on the energy scale in the panels d).

experimental TDPAC spectrum at room temperature, which was previously measured in coarse grained HfO₂ (Ref. 3, with author permission). Figure 2 shows the new fitted curve obtained by considering a CEMI. The obtained hyperfine parameters are summarized in Table II and compared with those reported in Ref. 3 for the case of two pure electric quadrupole interactions. The accuracy of the fit is comparable to that reported in Ref. 3. Independently of the model used for the second interaction, the fitted values corresponding to HFI1 remain unchanged. The other interaction (either HFI2 or HFI2C) represents mainly the anisotropy collapse of the TDPAC spectrum within a few nanoseconds, and in this way, it has not enough structure to be unambiguously fitted. However, as it can be seen from Table II, HFI2 and HFI2C are characterized by very similar high V_{ZZ} values.

Regarding the EFG, HFI2, and HFI2C are in agreement with our APW+lo prediction for both the nonspin-polarized and the spin-polarized calculations performed for the neutral charge state (see Table III). In the case of HFI2C, from the magnetic frequency $\omega_L = g_N \mu_N B_{hf} / h$ a magnetic hyperfine field of $B_{hf} = 11.2$ T is derived, which is in excellent agreement with the calculated one ($B_{hf}^{theor} = 11.8$ T). From all these results and the fact that APW+lo predicts that the spin-

polarized solution is energetically favorable, we conclude that the second interaction corresponds to Ta impurities probes located at Hf sites in a neutral charge state ($q=0$) with a net magnetic moment of about $0.35 \mu_B$ in the Ta sphere.

As already mentioned, some authors have reported ferromagnetism in pure HfO₂ thin films.^{2,20–22} In some papers the observed magnetism was associated with iron impurities while in others its origin was attributed to intrinsic defects of the material.^{20–23} One possible mechanism proposed for the observed magnetism is related to native oxygen vacancies, which act as donors, leading to the n -type doping of the material. However, in this case the magnetic interaction is negligible, and this rules out that hypothesis. In contrast, Hf vacancies show a high-spin state with an associated magnetic moment of about $3.5 \mu_B$.²² However, other groups argue that the hafnium vacancies are less likely to occur than the oxygen vacancies due to the high charge state.²³ It is also found that most of the ferromagnetism in HfO₂ is induced by the surface or the interface with the substrates instead of the bulk. The present calculation and the new interpretation of the experimental results indicate that the trapping of an electron at a cationic site can induce a magnetic moment local-

TABLE III. Calculated principal EFG component, V_{ZZ} , in units of 10^{21} V/m², asymmetry parameter η at the Ta impurity site and magnetic moments in the muffin-tin spheres of the Ta impurities (μ^{Ta}) and in the SC (μ^{SC}) for the different SC studied. ΔE denotes the energy difference (in eV) between the spin-polarized and nonspin-polarized solutions. The results were obtained by LSDA calculations. Spin polarization was not found in the case of $q=+1$.

		$q=0$		$q=+1$
		Spin-polarized	Nonspin-polarized	Nonspin-polarized
96-atom SC	$V_{ZZ}(\text{Ta site})$	+22.7	+20.0	+13.7
	$\eta(\text{Ta site})$	0.57	0.42	0.33
	μ^{SC}	1.00		
	μ^{Ta}	0.34		
	ΔE		-0.05	
192-atom SC	$V_{ZZ}(\text{Ta site})$	+22.5	+19.8	+13.6
	$\eta(\text{Ta site})$	0.58	0.40	0.32
	μ^{SC}	1.00		
	μ^{Ta}	0.35		
	ΔE		-0.13	
324-atom SC	$V_{ZZ}(\text{Ta site})$	+23.9	+20.1	+14.5
	$\eta(\text{Ta site})$	0.48	0.36	0.28
	μ^{SC}	1.00		
	μ^{Ta}	0.35		
	ΔE		-0.12	

ized at this site. This trapping effect could be related to the magnetism observed in thin films of pure HfO₂ since the surfaces could act as trapping centers. Further experiments and calculations will be very valuable in order to determine a possible magnetic ordering and the mechanism (or conditions) involved in a possible ferromagnetic behavior of HfO₂.

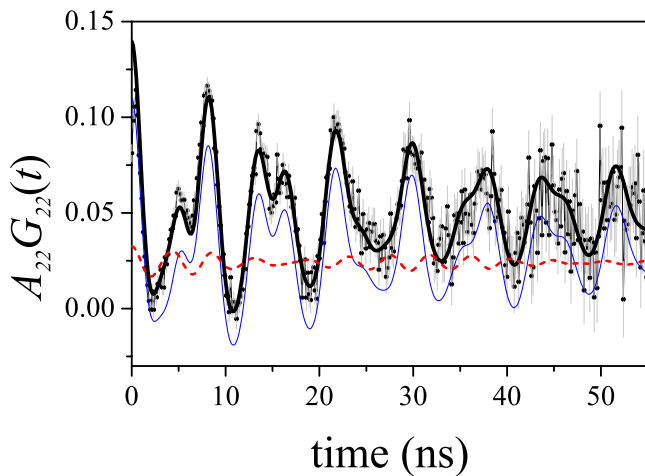


FIG. 2. (Color online) TDPAC spectrum of (Ta)HfO₂ at RT (Ref. 3) fitted with one electric quadrupolar interactions plus a CEMI. Solid black thick line is used for the sum of HF11 and HF12C while solid blue thin line is used for the HF11 contribution and dashed red line is used for HF12C.

IV. SUMMARY AND CONCLUSIONS

Density-functional calculations of the electronic structure and atomic forces have been used to examine monoclinic Ta-doped m -HfO₂ including spin-polarized calculations for different charge states. The force calculations were applied to optimize the doped structures relaxing all the atomic positions in the SC approximation. From the self-consistent potentials, hyperfine parameters at the Ta site were derived. The results were compared to the experimental TDPAC results reported in the literature and a new analysis of previous experimental results was performed.

The two experimentally detected hyperfine interactions were explained in terms of two different coexisting charge states for the Ta probe atom, giving an interpretation of the second hyperfine interaction at the Ta probe as originating from the $q=0$ charge state. This charge state corresponds to the trapping of one electron by the Ta impurity. In this charge state, the APW+lo calculations predict a net magnetic moment of $1.0 \mu_B$ in the SC ($0.35 \mu_B$ in the Ta muffin-tin sphere).

The results of the TDPAC experiments are compatible with the presence of a combined quadrupolar electrical +dipolar magnetic interactions. An excellent agreement between the experimental and theoretical magnetic hyperfine fields was obtained.

ACKNOWLEDGMENTS

This work was partially supported by Agencia Nacional de Promoción Científica y Tecnológica (ANPCyT) under

Grant No. PICT98 03-03727, Consejo Nacional de Investigaciones Científicas y Técnicas (CONICET) under Grants No. PEI6174 and No. PIP6032, Fundación/Antorchas, Argentina, and the Third World Academy of Sciences (TWAS), Italy, under Grant No. RGA 97-057. This research made use

of the HP-Parallel-Computing Bose Cluster and the computational facilities at IFLP and Departamento de Física (UNLP). Authors thank M Forker and M. Weissmann for fruitful discussion. We also thank M. Forker for permitting us to use TDPAC experimental results.

*Corresponding author; alonso.robertoe@gmail.com

- ¹R. E. Alonso, L. A. Errico, E. L. Peltzer y Blancá, A. López-García, A. Svane, and N. E. Christensen, *Phys. Rev. B* **78**, 165206 (2008).
- ²M. Venkatesan, C. B. Fitzgerald, and J. M. D. Coey, *Nature (London)* **430**, 630 (2004).
- ³M. Forker, P. de la Presa, W. Hoffbauer, S. Schlabach, M. Bruns, and D. V. Szabo, *Phys. Rev. B* **77**, 054108 (2008).
- ⁴G. Schatz and A. Weidinger, *Nuclear Condensed Matter Physics: Nuclear Methods and Applications* (Wiley, Chichester, England, 1996); E. N. Kaufmann and R. J. Vianden, *Rev. Mod. Phys.* **51**, 161 (1979); A. Lerf and T. Butz, *Angew. Chem., Int. Ed. Engl.* **26**, 110 (1987); H. Frauenfelder and R. M. Steffen, in *Alpha-, Beta-, and Gamma-Ray Spectroscopy*, edited by K. Siegbahn (North-Holland, Amsterdam, 1966), Vol. 2.
- ⁵T. Butz and A. Lerf, *Phys. Lett.* **97A**, 217 (1983).
- ⁶P. Raghavan, *At. Data Nucl. Data Tables* **42**, 189 (1989).
- ⁷M. Forker, R. Musseler, S. C. Bedi, M. Olzon-Dionysio, and S. D. de Souza, *Phys. Rev. B* **71**, 094404 (2005).
- ⁸P. de la Presa, M. Forker, J. T. Cavalcante, and A. P. Ayala, *J. Magn. Magn. Mater.* **306**, 292 (2006).
- ⁹A. Ayala, R. Alonso, and A. López-García, *Phys. Rev. B* **50**, 3547 (1994).
- ¹⁰H. Höhler, N. Atodiresei, K. Schroeder, R. Zeller, and P. H. Dederichs, *Phys. Rev. B* **71**, 035212 (2005); **70**, 155313 (2004).
- ¹¹E. Sjöstedt, L. Nordström, and D. J. Singh, *Solid State Commun.* **114**, 15 (2000); G. K. H. Madsen, P. Blaha, K. Schwarz, E. Sjöstedt, and L. Nordström, *Phys. Rev. B* **64**, 195134 (2001); see also S. Cottenier, *Density Functional Theory and the Family of (L)APW-Methods: A Step-by-Step Introduction* (KU Leuven, Belgium, 2002).
- ¹²P. Blaha, K. Schwarz, G. Madsen, D. Kvasnicka, and J. Luitz, *WIEN2k, An Augmented Plane Wave Plus Local Orbitals Program for Calculating Crystal Properties*, edited by K. Schwarz (Technical Universität Wien, Austria, 1999).
- ¹³J. P. Perdew and Y. Wang, *Phys. Rev. B* **45**, 13244 (1992).
- ¹⁴Z. Wu and R. E. Cohen, *Phys. Rev. B* **73**, 235116 (2006).
- ¹⁵K. Schwarz, C. Ambrosch-Draxl, and P. Blaha, *Phys. Rev. B* **42**, 2051 (1990).
- ¹⁶L. A. Errico, G. Fabricius, M. Rentería, P. de la Presa, and M. Forker, *Phys. Rev. Lett.* **89**, 055503 (2002).
- ¹⁷L. A. Errico, G. Fabricius, and M. Rentería, *Phys. Rev. B* **67**, 144104 (2003).
- ¹⁸E. L. Muñoz, A. W. Carbonari, L. A. Errico, H. M. Petrilli, and M. Rentería, *Hyp. Int.* **178**, 37 (2007).
- ¹⁹F. D. Brandão, M. V. B. Pinheiro, G. M. Ribeiro, G. Medeiros-Ribeiro, and K. Krambrock, *Phys. Rev. B* **80**, 235204 (2009).
- ²⁰J. M. D. Coey, M. Venkatesan, P. Stamenov, C. B. Fitzgerald, and L. S. Dorneles, *Phys. Rev. B* **72**, 024450 (2005).
- ²¹J. M. D. Coey, *J. Appl. Phys.* **97**, 10D313 (2005).
- ²²C. Das Pemmaraju and S. Sanvito, *Phys. Rev. Lett.* **94**, 217205 (2005).
- ²³H. Weng and J. Dong, *Phys. Rev. B* **73**, 132410 (2006).